Noncovalent Side-Chain Functionalization of Terpolymers

Clinton R. South,[†] Ken C.-F. Leung,[‡] Daniela Lanari,[‡] J. Fraser Stoddart,*[,‡] and Marcus Weck*[,†]

School of Chemistry and Biochemistry, Georgia Institute of Technology, Atlanta, Georgia 30332-0400, and California NanoSystems Institute & Department of Chemistry and Biochemistry, University of California, Los Angeles, 405 Hilgard Avenue, Los Angeles, California 90095

Received February 10, 2006; Revised Manuscript Received March 24, 2006

ABSTRACT: Random poly(norbornene)-based terpolymers containing sulfur−carbon−sulfur (SCS) palladated pincer complexes, dibenzo[24]crown-8 (DB24C8) rings, and diaminopyridine moieties were synthesized by ring-opening metathesis polymerization. Examination of the kinetics of the polymerization led to the conclusion that the polymerization of a statistical mixture of the three monomers results in the formation of random terpolymers. The terpolymers have molecular weights between 30 000 and 50 000 Da, with polydispersity indices ranging form 1.3 to 1.5, as determined by gel-permeation chromatography. Side-chain functionalization of these terpolymers was achieved by self-assembling (i) pyridines to the palladated pincer complexes, (ii) dibenzylammonium ions to the DB24C8 rings, and (iii) thymines to the diaminopyridine receptors. ^{1}H NMR spectroscopy was used to monitor the self-assembly processes and revealed that all self-assembly steps were fast and near quantitative. Isothermal titration calorimetry was employed to determine the association constants for the individual noncovalent functionalization steps. For all the self-assembly steps, the association constants were unaffected by neighboring functionalities on the polymer backbone, demonstrating orthogonality in the recognition expressed by the three recognition sites.

Introduction

Highly functionalized random terpolymers are desirable synthetic targets for a large variety of biological and electronic applications. In the context of biomaterials, terpolymers have been studied as potential drug carriers.[1] Terpolymers have also been used as cross-linking materials,[2] in curing applications,[2] and as molecular switches.[3] Recently, Krzysztof et al. reported "smart" polymeric nanospheres produced from random terpolymers that change their conformation in response to light exposure in solution.[3] Moreover, terpolymers are candidates for solution processable materials, such as photorefractive devices that require three components in order to become operational.[4]

Despite the importance of terpolymers in materials science, synthetic strategies to produce such materials are cumbersome and time-consuming since they have relied exclusively to date on covalent approaches. A more modular approach would be to employ noncovalent synthesis which has been shown[5−7] to be an efficient tool in the formation of supramolecular materials. Motivated by Nature's mechanisms, in which libraries of polymeric structures are produced by noncovalent-mediated synthesis,[8] we have developed functionalization strategies which use hydrogen bonding and metal coordination as tools for side-chain functionalization of well-defined random copolymers.[9,10] In this short account, we extend the complexity of our approach and report an efficient strategy for the functionalization of random terpolymers using self-assembly.

A requirement for the successful noncovalent functionalization of terpolymers is the selection of three molecular recognition motifs that can be assembled independently with their corresponding substrates. In our previously reported[10] two-component polymeric system, which was based on metal coordination and hydrogen bonding, we have shown that the two self-assembly events occur in an orthogonal manner. However, in a two-component system in which both the noncovalent functionalizations are based on hydrogen bonding, we found that competition between the different recognition motifs exists.[9] Thus, to achieve site-specific, noncompetitive, noncovalent functionalization of terpolymers, we designed a polymeric scaffold bearing three independent receptors that can be functionalized using metal coordination, pseudorotaxane formation, and hydrogen bond arrays. A graphical representation of the noncovalent functionalization strategy is shown in Figure 1. This approach toward terpolymer synthesis provides an attractive alternative to traditional terpolymer functionalization strategies based on covalent synthesis. It is an approach that (1) allows for rapid side-chain modification, (2) avoids lengthy postpolymerization purification steps, and (3) is reversible and therefore amenable to the rapid optimization of materials.

The metal coordination unit we have employed is based on the palladated sulfur−carbon−sulfur (SCS) pincer complex that can coordinate nitriles, pyridines, and phosphines.[11−13] The metalated pincer complex was chosen because of its high stability in nonpolar organic solvents.[12] Second, pseudorotaxane formation, based on the threading of dibenzylammonium ions into dibenzo[24]crown-8 (DB24C8) rings, is employed.[14−23] This interaction, which is highly specific with association constants in excess of 10^5 M^{-1} in CH_2Cl_2, involves the formation

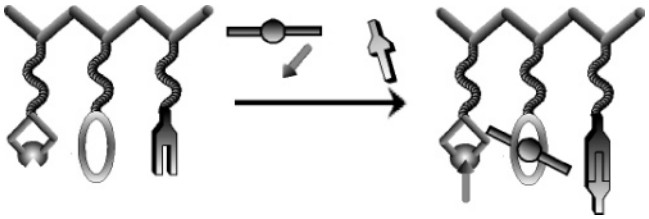

Figure 1. Graphical representation of the site-specific functionalization of random terpolymer.

[†] Georgia Institute of Technology.
[‡] University of California, Los Angeles.
* Corresponding authors. E-mail: stoddart@chem.ucla.edu, marcus.weck@chemistry.gatech.edu.

10.1021/ma060314s CCC: $33.50
Published on Web 05/03/2006

Scheme 1. Synthesis of Terpolymers[a]

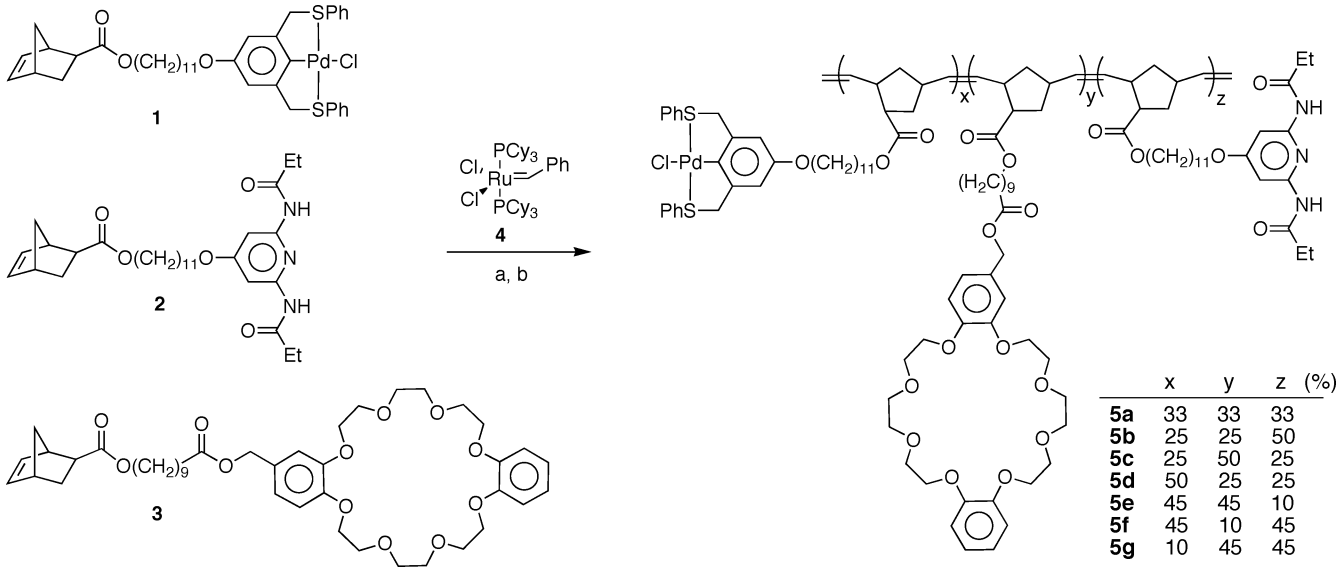

[a] (a) CH_2Cl_2, 4 h, 25 °C; (b) ethyl vinyl ether, 10 min. Ph− and EtO− end groups are omitted for clarity.

of strong [N^+−H···O] hydrogen bonds between the acidic NH_2^+ protons and the oxygen atoms in the DB24C8 ring. Moreover, additional [C−H···O] and $\pi-\pi$ stacking interactions as well as electrostatic forces also contribute to the stability of the pseudorotaxane formation. The third noncovalent recognition motif is based on the diaminopyridine and thymine donor−acceptor−donor hydrogen-bonding recognition pair that has already been used extensively in supramolecular polymer science.[5,10,13,24−26] The combination of these three recognition motifs along an architecturally controlled polymer backbone allows for fast and precise site-specific functionalization with a limited number of purification steps.

Results and Discussion

Polymer Synthesis. The terpolymers are based on norbornene monomers **1**−**3** bearing recognition motifs suitable for subsequent noncovalent modification. The synthesis and homopolymerization behavior by ring-opening metathesis polymerization (ROMP) of the three individual monomers have been reported before.[13,27] All terpolymers were synthesized according to Scheme 1 using the ruthenium initiator **4**, with varying amounts of monomers **1**−**3** resulting in terpolymers with varying densities of each recognition motif expressed along the polymer backbone. The recognition unit density was varied in order to determine whether the orthogonality of the noncovalent functionalization strategy is dependent on the individual functional group densities along the polymer backbone. The molecular weights of all the terpolymers were determined using gel-permeation chromatography (GPC). Controlled molecular weights were observed for all polymers regardless of the monomer feed ratios. GPC traces of all the terpolymers revealed monomodal distributions, ruling out the possibilities of homopolymerizations. Additionally, polydispersity indices (PDIs) ranged from 1.3 to 1.5 (Table 1), indicating well-behaved copolymerizations.

The statistical nature of the resulting terpolymers was examined on the basis of the polymerization kinetics of individual monomers as well as from the point of view of the terpolymerization kinetics. The rate of the polymerization for the DB24C8 monomer **3** was determined by in situ ^{1}H NMR spectroscopy and then compared to the previously measured rates of polymerization for the monomers **1** and **2**.[13b] The polymerization of a 20:1 ratio of monomer **3** to initiator **4** was complete after 20 min, as indicated by the shift of the norbornene olefin signals originating from $\delta = 6.17$ ppm (monomer) to $\delta = 5.38$ ppm (polymer). Figure 2 displays the kinetic plot for percentage conversion with time (top) and the corresponding logarithm plot (bottom) used to calculate the rate constant for the polymerization of monomer **3** in $CHCl_3$, using ruthenium initiator **4**. The pseudo-first-order rate constant for the polymerization of monomer **3** with [M] = 0.222 M and [I] = 0.0111 M was found to be 5.0×10^3 s^{-1}, a value which is comparable to the rate constants for the homopolymerizations of pincer monomer **1** (6.27×10^3 s^{-1}) and diaminopyridine monomer **2**

Table 1. GPC Data for Terpolymers[a]

terpolymer	M_n	M_w	PDI
5a	42 500	56 000	1.32
5b	32 400	44 700	1.38
5c	30 600	43 600	1.42
5d	31 400	44 400	1.41
5e	21 200	30 000	1.42
5f	30 700	44 600	1.45
5g	30 000	41 500	1.38

[a] Solvent: CH_2Cl_2.

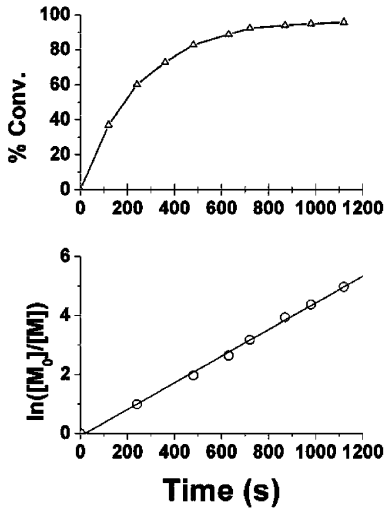

Figure 2. Kinetic plot of percentage conversion vs time (top) and the corresponding logarithm plot (bottom) for the polymerization of monomer **3**.

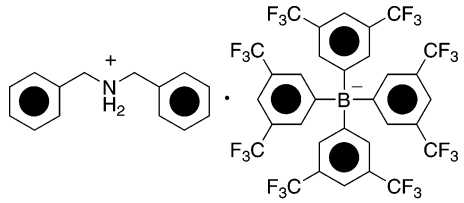

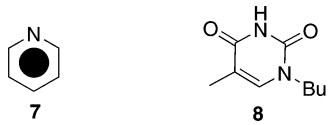

Figure 3. Functional units introduced onto the terpolymer receptors.

(6.51×10^3 s^{-1}).[13b] In addition, the in situ monitoring of terpolymerization by ^{1}H NMR spectroscopy revealed that all three monomers had undergone copolymerization within 20 min. Taking into account the fact that the polymerizable moiety for all three monomers is the same, these results prove that the copolymerization proceeded randomly instead of in a block copolymerization.

Self-Assembly Studies. Terpolymers **5a**−**g** used in this study are capable of undergoing self-assembly with their complementary substrates **6**−**8**, shown in Figure 3. The DB24C8 recognition moiety undergoes high-yielding pseudorotaxane formation with the dibenzylammonium ions **6-H·BAr$_F$**. The BAr$_F$ anion increases the binding affinity of the dibenzylammonium ion for the DB24C8 ring by forming a weakly associating salt with the ion, thereby increasing the charge density around the ammonium center. Pyridine (**7**) was chosen as the ligand for coordination with the Pd pincer complex because the coordination event can be characterized easily by ^{1}H NMR spectroscopy.[10] Finally, *N*-butylthymine (**8**) was chosen as the complementary substrate for the diaminopyridine receptor (**2**) because of the ease of characterizing the complex formed[10] and the increase in solubility compared to nonfunctionalized thymines.

Scheme 2 shows the stepwise functionalization of terpolymer **5a**. First, 1 equiv of pyridine (**7**) is added relative to the amount of Pd pincer complex in the terpolymer **5a**, followed by the addition of 1 equiv of $AgBF_4$. Upon the formation of the cationic Pd species,[12,13] i.e., the availability of an open coordination site on the Pd, the pyridine unit coordinates rapidly to the Pd−pincer complex, forming the monofunctional terpolymer {**5a·(7·BF$_4$)$_n$**}$^{n+}$. Subsequently, the dibenzylammonium salt **6-H·BAr$_F$** is added to the terpolymer {**5a·(7·BF$_4$)$_n$**}$^{n+}$, and pseudorotaxane formation ensues, forming the bifunctional {**5a·[(6-H·BAr$_F$)-(7·BF$_4$)]$_n$**}$^{2n+}$. Finally, after the addition of *N*-butylthymine (**8**)-to terpolymer {**5a·[(6-H·BAr$_F$)(7·BF$_4$)]$_n$**}$^{2n+}$, the trifunctional terpolymer {**5a·[(6-H·BAr$_F$)(7·BF$_4$)(8)]$_n$**}$^{2n+}$ is obtained.

Proton NMR spectroscopy was used to monitor the self-assembly processes. Figure 4A shows the ^{1}H NMR spectrum of terpolymer **5a**, while Figure 4B shows a mixture of terpolymer **5a** and pyridine (**7**) that are present in a 1:1 ratio with the pincer complexes present along the terpolymer. Initially, no signal shifts are observed after the addition of pyridine **7** to **5a**. Subsequently, after the addition of $AgBF_4$ to the mixture, **7** coordinates quantitatively to the Pd centers to form the monofunctional terpolymer {**5a·(7·BF$_4$)$_n$**}$^{n+}$ (Figure 4C). The coordination of the pyridine ligands to the terpolymer **5a** is reflected in the characteristic upfield shift of the α-pyridyl signal (H_b) from $\delta = 8.59$ ppm to $\delta = 8.14$ ppm.[28] In addition to this diagnostic shift of the α-pyridyl proton signals, the signal of the methylene arms on the pincer (labeled H_a in Figure 4) sharpens and shifts downfield (Figure 4C) from $\delta = 4.62$ ppm

Scheme 2. Noncovalent Functionalization of Terpolymers[a]

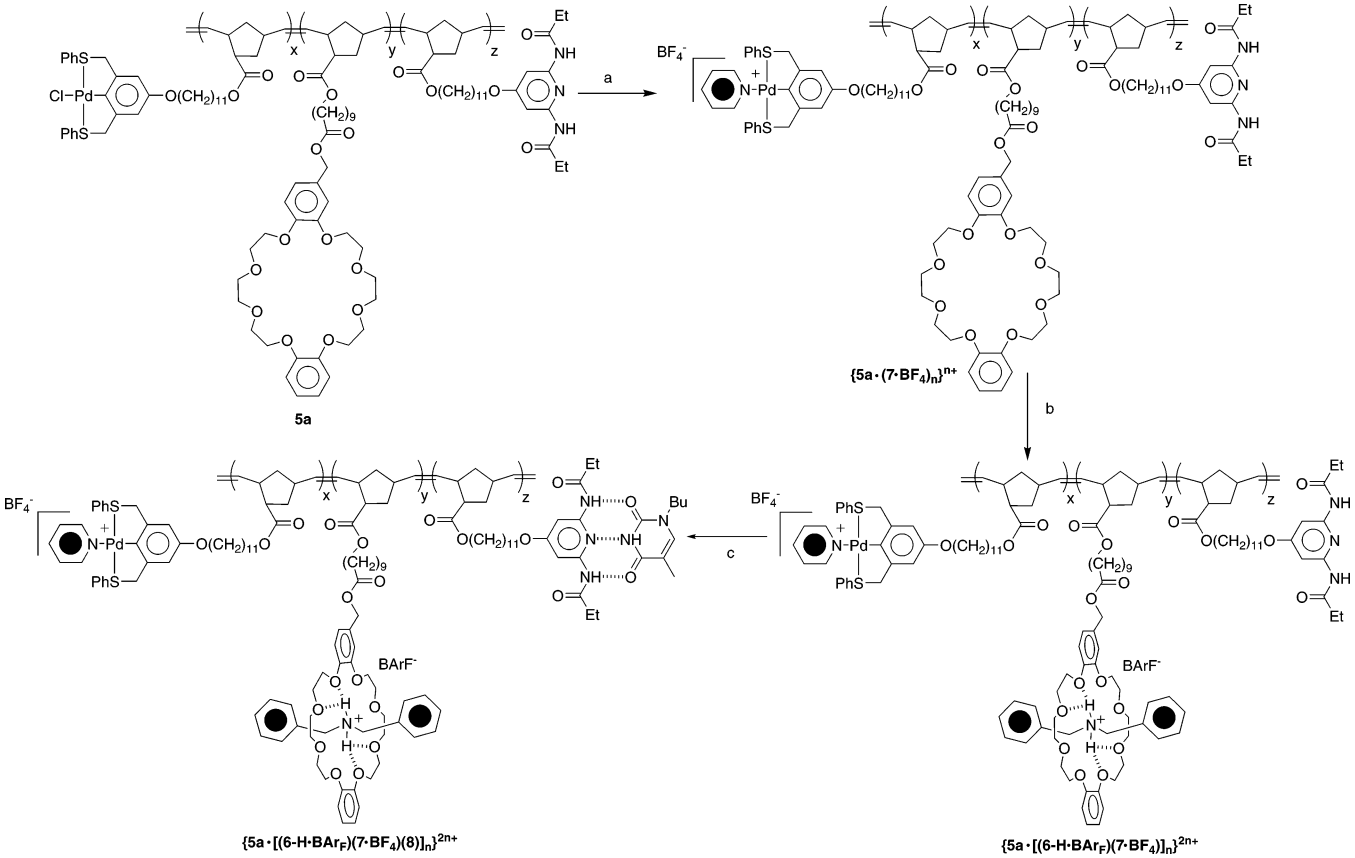

[a] (a) **7**, $AgBF_4$; (b) **6-H·BAr$_F$**; (c) 1.5 equiv of **8** (solvent = CD_2Cl_2).

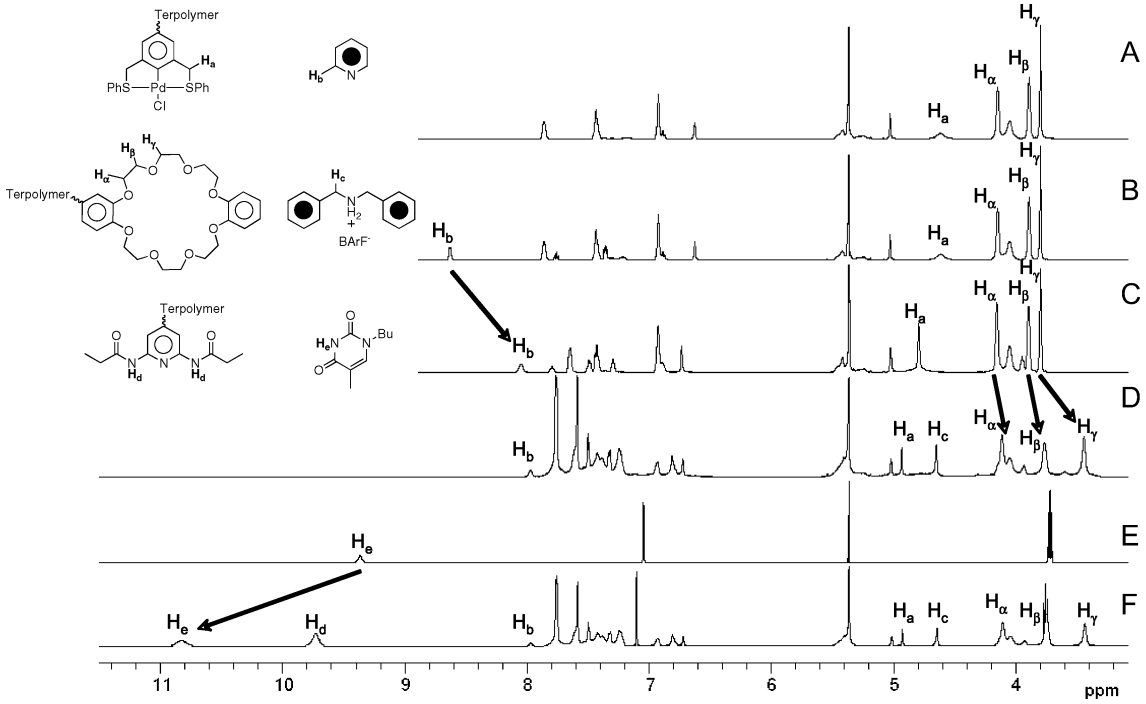

Figure 4. Partial ^{1}H NMR spectra (500 MHz) with the corresponding legend depicting the self-assembly of terpolymer **5a** in CD_2Cl_2 at 25 °C: (A) terpolymer **5a**; (B) terpolymer **5a** with 1 equiv of pyridine (**7**) (not assembled); (C) monofunctional terpolymer $\{\mathbf{5a\cdot(7\cdot BF_4)}_n\}^{n+}$ (after the addition of $AgBF_4$ to the mixture of **5a** and **7**); (D) bifunctional terpolymer $\{\mathbf{5a\cdot[(6\text{-}H\cdot BAr_F)(7\cdot BF_4)]}_n\}^{2n+}$ (after the addition of **6-H·BAr$_F$** to $\{\mathbf{5a\cdot(7\cdot BF_4)}_n\}^n$); (E) reference spectra of *N*-butylthymine (**8**); (F) fully trifunctionalized terpolymer $\{\mathbf{5a\cdot[(6\text{-}H\cdot BAr_F)(7\cdot BF_4)(8)]}_n\}^{2n+}$ after the addition of 1.5 equiv of **8** to $\{\mathbf{5a\cdot[(6\text{-}H\cdot BAr_F)(7\cdot BF_4)]}_n\}^{2n}$.

to $\delta = 4.75$ ppm. Furthermore, after the addition of 1 equiv of **6-H·BAr$_F$** to the monofunctional terpolymer $\{\mathbf{5a\cdot(7\cdot BF_4)}_n\}^{n+}$, pseudorotaxane formation ensues, and the bifunctional terpolymer $\{\mathbf{5a\cdot[(6\text{-}H\cdot BAr_F)(7\cdot BF_4)]}_n\}^{2n+}$ forms (Figure 4D). The threading event results in diagnostic shifts of numerous of proton resonance signals in the ^{1}H NMR spectrum (Figure 4D). The signals of the α, *β*, and *γ* protons in the DB24C8 ring shift upfield from $\delta = 4.18$, 3.88, and 3.79 ppm to $\delta = 4.13$, 3.85, and 3.41 ppm, respectively. Moreover, the benzylic methylene protons (labeled H_c in Figure 4) adjacent to the ammonium center appear at $\delta = 4.62$ ppm, indicating that the dibenzylammonium ions are encircled by the DB24C8 rings.[29] Furthermore, upon pseudorotaxane formation, a slight upfield shift of the α-pyridyl signal from $\delta = 8.14$ to 7.99 ppm and a downfield shift of the pincer methylene protons from $\delta = 4.74$ to 4.65 ppm occurs (Figure 4D). These shifts are indicative of a stronger coordinative bond between the pyridine ligand and the pincer complex,[28] a situation which is presumably a result of BF_4^-/BAr_F^- counterion exchange, since the nature of the outer-sphere anion present in Pd−pincer complexes has been shown to create conformational changes in the coordinated ligand, thereby affecting its magnetic environment.[30] To verify this hypothesis, control experiments on homopolymer **1** were carried out in which $NaBAr_F$ and/or dibenzylammonium BAr_F were added to the polymer after the coordination of **7**. In both cases, upfield shifts of the α-pyridyl signals and downfield shifts of the pincer methylene proton signals were observed. These shifts are analogous to the shifts observed during the noncovalent terpolymer functionalization. These results indicate that counterion exchange occurs along the polymer backbone during functionalization. However, such an exchange does not interfere with the integrity of the Pd−pyridine bond during the formation of pseudorotaxanes, proving the orthogonality of these two noncovalent interactions along the terpolymers.

Finally, to obtain the fully loaded functional terpolymer $\{\mathbf{5a\cdot[(6\text{-}H\cdot BAr_F)(7\cdot BF_4)(8)]}_n\}^{2n+}$, 1 equiv of *N*-butylthymine (**8**) is added to the bifunctional terpolymer $\{\mathbf{5a\cdot[(6\text{-}H\cdot BAr_F)(7\cdot BF_4)]}_n\}^{2n+}$. The ^{1}H NMR spectrum (Figure 4F) of the resulting functional terpolymer $\{\mathbf{5a\cdot[(6\text{-}H\cdot BAr_F)(7\cdot BF_4)(8)]}_n\}^{2n+}$ (Figure 4E,F) shows a downfield shift of the imide signal of *N*-butylthymine from $\delta = 9.40$ ppm to $\delta = 10.81$ ppm. Moreover, the amide signals of the diaminopyridine units, which were not resolved in the bifunctional terpolymer $\{\mathbf{5a\cdot[(6\text{-}H\cdot BAr_F)(7\cdot BF_4)]}_n\}^{2n+}$, appear (Figure 4F) characteristically[24] upon hydrogen bonding at $\delta = 9.85$ ppm (Figure 4F). Consequently, the ^{1}H NMR spectroscopic studies reveal that the stepwise terpolymer functionalization is achieved without affecting the molecular recognition of the next receptor. Analogous chemical shifts upon the stepwise functionalization of all the terpolymers, i.e. **5b**−**g**, were observed in the ^{1}H NMR spectra.

Isothermal titration calorimetry (ITC) was used to determine the relative binding affinities for the three different self-assembly processes. The single-site binding constant for a ligand X binding to a polymer is given by the equation K_a = [unfilled sites]/([filled sites][X]).[31] Each binding event along the terpolymer is therefore treated as independent, and apparent single-site association constants are calculated using the thermodynamic parameters obtained from ITC measurements. The shape of the binding isotherms can provide valuable qualitative information about relative binding strengths. Figure 5 shows a stack plot of two example isotherms gathered upon the titration of appropriate substrates into a solution of a terpolymer receptor. The top isotherm in Figure 5 is an example of very strong binding, while the bottom one is characteristic of a much weaker binding event. The top isotherm shows strong binding between the dibenzylammonium salt **6-H·BAr$_F$** and the terpolymer **5a**, where intense signals for an exothermic process are observed until the saturation point is reached. By contrast, the bottom

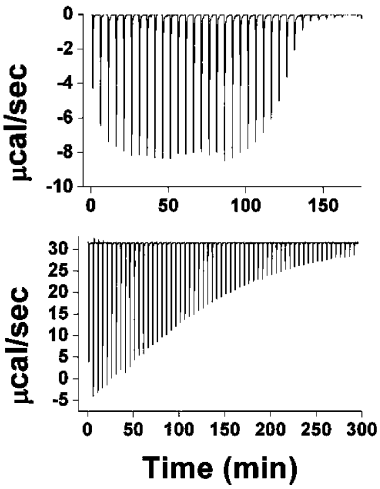

Figure 5. Example ITC binding isotherms with strong binding of **6-H·BAr$_F$** (top) and weak binding of **8** with terpolymer **5a** (bottom) in CH_2Cl_2 solutions.

isotherm is characteristic of a weaker binding event between *N*-butylthymine (**8**) and the terpolymer **5a**.

Association constants (K_a), which can be employed for relative comparisons, for the terpolymer functionalization were calculated from the corresponding binding isotherms (Table 2) such as the ones represented in Figure 5. For terpolymers **5a**−**g**, the K_a value for coordinating pyridine (**7**) to the Pd−pincer complexes was found to be larger than 10^9 M^{-1}. Upon the titration of pyridine (**7**) into terpolymers **5a**−**g**, a heat saturation curve was observed, indicating the upper sensitivity level ($>10^9$ M^{-1}) of the ITC instrument has been reached. Strong binding isotherms are also observed upon the titration of **6-H·BAr$_F$** with the terpolymers **5a**−**g**. Association constants for the pseudorotaxane formation range from 170 000 to 450 000 M^{-1}. In all cases, however, the binding of the dibenzylammonium ion of the salt **6-H·BAr$_F$** with the DB24C8 rings on the terpolymers resulted in very tight binding, indicating near-quantitative functionalization.

Lower K_a values are observed for the self-assembly process between **8** and the diaminopyridines on the terpolymers. For this self-assembly process, association constants ranging from 1400 to 1700 M^{-1} with only slight changes in association constants between terpolymers **5a**−**g** were measured. The small changes observed are within the experimental error limits, suggesting that the K_a value for the hydrogen bonding event is independent of the terpolymer composition.

Finally, the K_a values for the orthogonal recognition motifs were measured in order to show that the binding by subsequent receptor units is not affected by the presence of previously assembled ligands. The association constant for the pseudorotaxane formation between terpolymer $\{\mathbf{5a}\cdot(\mathbf{7}\cdot\mathbf{BF_4})_n\}^{n+}$ and **6-H·BAr$_F$** was found to be 310 000 M^{-1}, a value which is well within the range of other K_a values obtained among terpolymers **5a**−**g**, indicating that the assembled pyridine unit does not interfere with the formation of the pseudorotaxane. Furthermore, once both strong substrates like **7** and **6-H·BAr$_F$** are assembled onto terpolymer **5a**, the subsequent binding of *N*-butylthymine (**8**) with the diaminopyridine receptor to produce the fully functional terpolymer $\{\mathbf{5a}\cdot[(\mathbf{6\text{-}H}\cdot\mathbf{BAr_F})(\mathbf{7}\cdot\mathbf{BF_4})(\mathbf{8})]_n\}^{2n+}$ is not affected (Table 2) by either of these two binding events. The measured association constant for the hydrogen-bonding self-assembly was 1570 M^{-1}, a value close to the K_a values measured for nonfunctionalized systems. These results indicate that the terpolymers can be functionalized in an orthogonal and stepwise fashion without compromising the integrity of neighboring interactions.

Table 2. Association Constants Measured by ITC[a]

terpolymer	K_a[b] (M^{-1})	K_a[c] (M^{-1})
5a	231 000	1600
5b	423 000	1520
5c	345 000	1760
5d	174 000	1650
5e	459 000	1440
5f	399 000	1260
5g	325 000	1400
$\{\mathbf{5a}\cdot(\mathbf{7}\cdot\mathbf{BF_4})_n\}^n$	310 000	
$\{\mathbf{5a}\cdot[(\mathbf{6\text{-}H}\cdot\mathbf{BAr_F})(\mathbf{7}\cdot\mathbf{BF_4})]_n\}^{2n+}$		1570

[a] Values determined in CH_2Cl_2 at 298 K. [b] K_a for the complexation with **6-H·BAr$_F$**. [c] K_a for the complexation with **8**.

Conclusions

A noncovalent functionalization strategy for terpolymers based on self-assembly processes has been developed. The highly controlled terpolymerization of three different functional norbornene monomers bearing recognition motifs was successfully achieved by ROMP. An investigation of the kinetics of the polymerization of the three monomers revealed that statistical random terpolymers are formed during the controlled polymerization. Noncovalent functionalization of the terpolymers was achieved by the introduction of (i) pyridine units into Pd−pincer complexes, (ii) dibenzylammonium ions into DB24C8 rings, and (iii) *N*-butylthymines to the diaminopyridines. ^{1}H NMR spectroscopic characterization of the self-assembly events indicates that the three noncovalent interactions act independently of each other and demonstrates that the functionalization strategy can be applied to terpolymers in a stepwise fashion. Isothermal titration calorimetry was employed to determine the strength of these noncovalent interactions. The results show that the binding of recognition pairs is not affected by the composition of the terpolymer backbone and that functionalization can be achieved in an orthogonal manner without decreasing the binding affinities of the receptors attached to the polymer backbone. Eventually, this noncovalent functionalization strategy will be useful for creating materials for various applications that require extensive screening and rapid materials optimization. The approach we are describing requires polymer characterization of only a single, generic backbone that can be shelved and used for several different purposes. Such a generic backbone may provide a gateway to a combinatorial approach to polymer synthesis. Efforts to expand on this methodology are currently being studied in our laboratories.

Experimental Section

General Methods. All reagents were purchased either from Acros Organics, Aldrich, or Strem Chemicals and used without further purification unless otherwise noted. CH_2Cl_2 was dried via passage through copper oxide and alumina columns. NMR spectra were recorded using a 500 MHz Bruker DRX spectrometer (^{1}H NMR: 500 MHz; ^{13}C NMR: 125 MHz). Spectra were referenced from the residual proton of the deuterated solvent. Gel-permeation chromatography analyses were carried out at room temperature using a Waters 1525 binary pump coupled to a Waters 2414 refractive index detector with CH_2Cl_2 as the eluant and a flow rate of 1 mL/min on American Polymer Standards 10 μm particle size, linear mixed bed packing columns. Gel-permeation chromatograms were calibrated using poly(styrene) standards. Isothermal titration calorimetry was performed on a Microcal VP-ITC isothermal calorimeter. Degassed, HPLC grade CH_2Cl_2 was used for all ITC experiments. Monomers **1**,[13] **2**,[13] and **3**,[27] and compounds **6-H·BAr$_F$**[27] and **8**[24] were synthesized according to the previously published procedures.

The preparation chemistry involving terpolymer **5a** is given as an example for all copolymerizations and polymer functionalizations.

Terpolymer 5a. Monomers **1** (20 mg, 0.03 mmol), **2** (14 mg, 0.03 mmol), and **3** (20 mg, 0.03 mmol) were dissolved in anhydrous, degassed CH_2Cl_2 under an argon atmosphere. The ruthenium initiator **4** (2.47 mg, 0.003 mmol) was added as a solution in CH_2Cl_2. Upon complete polymerization, a drop of ethyl vinyl ether was added to quench the polymerization. The terpolymer **5a** was isolated by repeated precipitations into cold MeOH (52 mg, 97%). ^{1}H NMR (CD_2Cl_2): δ = 8.00 (m, 4H), 7.58 (m, 6H), 7.37 (s, 2H), 7.01 (m, 7H), 6.69 (m, 2H), 5.55−5.31 (m, 6H), 5.12 (s, 2H), 4.77 (s, 4H), 4.31 (m, 8H), 4.10 (m, 6H), 3.98 (m, 8H), 3.83 (m, 8H), 3.22−3.00 (m, 6H), 3.05−1.87 (m, 83H). ^{13}C NMR ($CDCl_3$): δ = 176.0, 173.8, 150.5, 149.4, 149.3, 133.0, 131.8, 130.3, 129.9, 121.9, 121.8, 114.9, 114.7, 114.2, 109.2, 71.4, 70.2, 70.2, 69.7, 69.6, 68.5, 66.2, 64.8, 52.2, 50.0, 34.6, 29.9, 29.8, 29.7, 29.5, 29.1, 26.4, 26.3, 25.3.

Terpolymer $\{\mathbf{5a{\cdot}(7{\cdot}BF_4)}_n\}^{n+}$. Terpolymer **5a** (50 mg) was dissolved in CH_2Cl_2 or CD_2Cl_2, and pyridine (**7**) was added until a 1:1 equivalency was reached in relation to the Pd−pincer complexes as determined by ^{1}H NMR spectroscopy. One equivalent of $AgBF_4$ dissolved in $MeNO_2$ was added to the reaction mixture. After stirring for 5 min, the precipitated AgCl(s) was removed by centrifugation. The supernatant liquid was filtered through a plug of Celite and subsequently through a 0.45 μm syringe filter. The solvent was removed in vacuo to yield the monofunctional terpolymer $\{\mathbf{5a{\cdot}(7{\cdot}BF_4)}_n\}^{n+}$ as an orange solid (yield: 100%). ^{1}H NMR (CD_2Cl_2): δ = 8.14 (s, 2H), 7.89 (m, 3H), 7.73 (m, 4H), 7.56 (m, 6H), 7.37 (s, 2H), 7.04 (m, 6H), 6.79 (m, 2H), 5.55−5.31 (m, 6H), 5.09 (s, 2H), 4.91 (s, 4H), 4.31 (m, 8H), 4.10 (m, 6H), 3.98 (m, 8H), 3.83 (m, 8H), 3.22−3.00 (m, 6H), 3.05−1.87 (m, 83H). ^{13}C NMR ($CDCl_3$): δ = 176.0, 173.8, 150.5, 149.5, 149.4, 149.3, 133.0, 130.8, 130.7, 130.3, 129.9, 121.8, 121.7, 121.5, 114.9, 114.7, 114.2, 109.2, 71.5, 70.2, 70.1, 69.7, 69.6, 68.5, 66.2, 64.8, 52.2, 50.0, 34.6, 29.9, 29.8, 29.6, 29.5, 29.1, 26.4, 26.3, 25.3.

Terpolymer $\{\mathbf{5a{\cdot}[(6\text{-}H{\cdot}BAr_F)(7{\cdot}BF_4)]}_n\}^{2n+}$. Terpolymer $\{\mathbf{5a{\cdot}(7{\cdot}BF_4)}_n\}^{n+}$ (50 mg) was dissolved in CH_2Cl_2, and 1 equiv of the dibenzylammonium salt **6-H·BAr$_F$** was added. Upon stirring the solution for 10 min, the solvent was removed in vacuo to yield the bifunctional terpolymer $\{\mathbf{5a{\cdot}[(6\text{-}H{\cdot}BAr_F)(7{\cdot}BF_4)]}_n\}^{2n+}$ as an orange solid (yield: 100%). ^{1}H NMR (CD_2Cl_2): δ = 8.08 (s, 2H), 7.89 (m, 11H), 7.73 (m, 4H), 7.70 (m, 4H) 7.54 (m, 6H), 7.36 (s, 2H), 7.02 (s, 6H), 6.86 (m, 2H), 6.75 (m, 2H), 5.55−5.31 (m, 6H), 5.07 (s, 2H), 4.95 (s, 4H), 4.73 (s, 4H), 4.32 (m, 8H), 4.10 (m, 6H), 3.85 (m, 8H), 3.61 (m, 8H), 3.22−3.00 (m, 6H), 3.05−1.87 (m, 83H). ^{13}C NMR (CD_2Cl_2): δ = 176.0, 173.8, 150.5, 149.5, 149.4, 149.3, 147.8, 135.2, 133.0, 132.1, 130.8, 130.7, 130.2, 130.0, 129.6, 129.0, 122.0, 121.8, 121.7, 121.5, 114.9, 114.7, 114.2, 109.2, 71.5, 71.0, 70.6, 70.2, 70.2, 69.7, 69.6, 68.6, 68.5, 66.2, 64.8, 52.2, 50.0, 34.6, 29.9, 29.8, 29.6, 29.5, 29.1, 26.4, 26.3, 25.3.

Terpolymer $\{\mathbf{5a{\cdot}[(6\text{-}H{\cdot}BAr_F)(7{\cdot}BF_4)(8)]}_n\}^{2n+}$**.** Terpolymer $\{\mathbf{5a{\cdot}[(6\text{-}H{\cdot}BAr_F)(7{\cdot}BF_4)]}_n\}^{2n+}$ (50 mg) was dissolved in CH_2Cl_2, and 1.5 equiv of *N*-butylthymine (**8**) was added. Upon stirring the solution for 10 min, the solvent was removed in vacuo to yield the trifunctional terpolymer $\{\mathbf{5a{\cdot}[(6\text{-}H{\cdot}BAr_F)(7{\cdot}BF_4)(8)]}_n\}^{2n+}$ as an orange solid (yield: 100%). ^{1}H NMR (CD_2Cl_2): δ = 10.80 (s, 1H), 9.65 (s, 2H), 8.08 (s, 2H), 7.89 (m, 11H), 7.73 (m, 4H), 7.70 (m, 4H) 7.54 (m, 6H), 7.36 (s, 2H), 7.15 (m, 2H) 7.02 (s, 6H), 6.86 (m, 2H), 6.75 (m, 2H), 5.55−5.31 (m, 6H), 5.07 (s, 2H), 4.95 (s, 4H), 4.73 (s, 4H), 4.32 (m, 8H), 4.10 (m, 6H), 3.85 (m, 8H), 3.76 (t, 2H, J = 6.5 Hz), 3.61 (m, 8H), 3.22−3.00 (m, 6H), 3.05−1.87 (m, 89H). ^{13}C NMR (CD_2Cl_2): δ = 177.0, 176.0, 173.8, 164.9, 162.7, 162.3, 161.9, 161.5, 151.4, 150.6, 147.8, 146.3, 141.1, 135.1, 132.3, 131.8, 131.5, 130.7, 130.3, 129.6, 129.4, 129.1, 129.0, 128.2, 126.5, 126.1, 123.9, 122.1, 117.9, 113.4, 113.1, 112.8, 110.5, 94.6, 71.0, 70.6, 68.7, 68.6, 68.6, 66.0, 64.8, 53.1, 48.5, 34.6, 31.4, 30.5, 30.1, 29.9, 29.7, 29.1, 26.3, 26.1, 25.3.

Acknowledgment. Financial support has been provided by the Office of Naval Research (MURI, Award N00014-03-1-0793) and the National Science Foundation (CHE-0239385). M.W. gratefully acknowledges a 3M Untenured Faculty Award, a DuPont Young Professor Award, an Alfred P. Sloan Fellowship, a Camille Dreyfus Teacher-Scholar Award, and the Blanchard Assistant Professorship.

References and Notes

(1) Wamsley, A.; Bhaskara, J.; Phiasivongsa, P.; Xiaoling, L. *J. Polym. Sci., Part A: Polym. Chem.* **2004**, *42*, 317−325.
(2) El-Ghayoury, A.; Harald, H.; de Ruiter, B.; Schubert, U. S. *Macromolecules* **2003**, *36*, 3955−3959.
(3) Krzysztof, S.; Jankowska, M.; Nowakowska, M. *J. Mater. Sci.: Mater. Med.* **2003**, *14*, 699−703.
(4) Bratcher, M. S.; DeClue, M. S.; Grunnet-Jepsen, A.; Wright, D.; Smith, B. R.; Moerner, W. E.; Siegel, J. S. *J. Am. Chem. Soc.* **1998**, *120*, 9680−9681.
(5) Pollino, J. M.; Weck, M. *Chem. Soc. Rev.* **2005**, *34*, 193−207.
(6) Brunsveld, L.; Folmer, B.; Meijer, E. W.; Sijbesma, R. P. *Chem. Rev.* **2001**, *101*, 4071−4098.
(7) Lehn, J.-M. *Supramolecular Chemistry*; Wiley-VCH: New York, 1995.
(8) Philp, D.; Stoddart, J. F. *Angew. Chem., Int. Ed. Engl.* **1996**, *35*, 1154−1196.
(9) Burd, C.; Weck, M. *Macromolecules* **2005**, *38*, 7225−7230.
(10) Pollino, J. M.; Stubbs, L. P.; Weck, M. *J. Am. Chem. Soc.* **2004**, *126*, 563−567.
(11) For discussions of pincer-type complexation see: (a) Crabtree, R. H. *Pure Appl. Chem.* **2003**, *75*, 435−443. (b) van Manen, H.-J.; Nakashima, K.; Shinkai, S.; Kooijman, H.; Spek, A. J.; van Veggel, F. C. J. M.; Reinhoudt, D. N. *Eur. J. Inorg. Chem.* **2000**, 2533−2540.
(12) (a) Albrecht, M.; Lutz, M.; Antoine, M. M.; Lutz, E. T. H.; Spek, A. L.; van Koten, G. *J. Chem. Soc., Dalton Trans.* **2000**, 3797−3804. (b) Albrecht, M.; van Koten, G. *Angew. Chem., Int. Ed.* **2001**, *40*, 3750−3781. (c) Albrecht, M.; van Koten, G. *Angew. Chem., Int. Ed.* **2001**, *40*, 3750−3781.
(13) For examples of Pd−pincer complexes in supramolecular chemistry see: (a) Pollino, J. M.; Weck, M. *Org. Lett.* **2002**, *4*, 753−756. (b) Pollino, J. M.; Stubbs, L. P.; Weck, M. *Macromolecules* **2003**, *36*, 2230−2234. (c) Yount, W. C.; Loveless, D. M.; Craig, S. L. *Angew. Chem., Int. Ed.* **2005**, *44*, 2746−2748. (d) Meijer, M. D.; Mulder, B.; van Klink, G. P. M.; van Koten, G. *Inorg. Chim. Acta* **2003**, *352*, 247−252. (e) Huck, W. T. S.; Prins, L. J.; Fokkens, R. H.; Nibbering, N. M. M.; van Veggel, F. C. J. M.; Reinhoudt, D. N. *J. Am. Chem. Soc.* **1998**, *120*, 6240−6246.
(14) (a) Ashton, P. R.; Chrystal, E. J. T.; Glink, P. T.; Menzer, S.; Schiavo, C.; Spencer, N.; Stoddart, J. F.; Tasker, P. A.; White, A. J. P.; Williams, D. J. *Chem.−Eur. J.* **1996**, *2*, 709−728. (b) Ashton, P. R.; Fyfe, M. C. T.; Raymo, F. M.; Spencer, N.; Stoddart, J. F.; White, A. J. P.; Williams, D. J. *J. Am. Chem. Soc.* **1998**, *120*, 2297−2307. (c) Ashton, P. R.; Ballardini, R.; Balzani, V.; Baxter, I.; Credi, A.; Fyfe, M. C. T.; Gandolfi, M. T.; Gómez-López, M.; Martínez-Díaz, Morosini, M.; Schiavo, C.; Shibata, K.; Stoddart, J. F.; White, A. J. P.; Williams, D. J. *Chem.−Eur. J.* **1998**, *4*, 2332−2341. (d) Fitzmaurice, D.; Rao, S. N.; Preece, J. A.; Stoddart, J. F.; Wenger, S.; Zaccheroni, N. *Angew. Chem., Int. Ed.* **1999**, *38*, 1147−1150.
(15) (a) Glink, P. T.; Schiavo, C.; Stoddart, J. F.; Williams, D. J. *Chem. Commun.* **1996**, 1483−1490. (b) Fyfe, M. C. T.; Stoddart, J. F. *Adv. Supramol. Chem.* **1999**, *5*, 1−53. (c) Fyfe, M. C. T.; Stoddart, J. F. *Coord. Chem. Rev.* **1999**, *183*, 139−155. (d) Fyfe, M. C. T.; Stoddart, J. F.; Williams, D. J. *Struct. Chem.* **1999**, *10*, 243−259. (e) Cantrill, S. J.; Pease, A. R.; Stoddart, J. F. *J. Chem. Soc., Dalton Trans.* **2000**, 3715−3734.
(16) (a) Hubin, T. J.; Kolchinski, A. G.; Vance, A. L.; Busch, D. H. *Adv. Supramol. Chem.* **1999**, *5*, 237−357. (b) Hubin, T. J.; Busch, D. H. *Coord. Chem. Rev.* **2000**, *200−202*, 5−52. (c) Clifford, T.; Abushamleh, A.; Busch, D. H. *Proc. Natl. Acad. Sci. U.S.A.* **2002**, *99*, 4830−4836.
(17) (a) Takata, T.; Kawasaki, H.; Kihara, N.; Furusho, Y. *Macromolecules* **2002**, *34*, 5449−5456. (b) Tachibana, Y.; Kihara, N.; Furusho, Y.; Takata, T. *Org. Lett.* **2004**, *6*, 4507−4509.
(18) (a) Yamaguchi, N.; Hamilton, L. M.; Gibson, H. W. *Angew. Chem., Int. Ed.* **1998**, *37*, 3275−3279. (b) Bryant, W. S.; Guzei, I. A.; Rheingold, A. L.; Merola, J. S.; Gibson, H. W. *J. Org. Chem.* **1998**, *63*, 7634−7639. (c) Yamaguchi, N.; Gibson, H. W. *Angew. Chem., Int. Ed.* **1999**, *38*, 143−147. (d) Gibson, H. W.; Yamaguchi, N.; Hamilton, L.; Jones, J. W. *J. Am. Chem. Soc.* **2003**, *125*, 3522−3533. (f) Jones, J. W.; Huang, F. H.; Bryant, W. S.; Gibson, H. W. *Tetrahedron Lett.* **2004**, *45*, 5961−5963.
(19) (a) Montalti, M.; Prodi, L. *Chem. Commun.* **1998**, 1461−1462. (b) Ishow, E.; Credi, A.; Balzani, V.; Spadola, F.; Mandolini, L. *Chem.−Eur. J.* **1999**, *5*, 984−989.

(20) (a) Duggan, S. A.; Fallon, G.; Langford, S. J.; Lau, V. L.; Satchell, J. F.; Paddon-Row, M. N. *J. Org. Chem.* **2001**, *66*, 4419−4426. (b) Langford, S. J.; Lau, V. L. *Aust. J. Chem.* **2004**, *57*, 29−32.
(21) Kawano, S. I.; Fujita, N.; Shinkai, S. *Chem. Commun.* **2003**, 1352−1353.
(22) (a) Chiu, S.-H.; Liao, K. S.; Su, J. K. *Tetrahedron Lett.* **2004**, *45*, 213-216. (b) Cheng, P. N.; Hung, W. C.; Chiu, S.-H. *Tetrahedron Lett.* **2005**, *46*, 4239−4242.
(23) Feng, D. J.; Li, X. Q.; Wang, X. Z.; Jiang, X. K.; Li, Z. T. *Tetrahedron* **2004**, *60*, 6137−6144.
(24) Stubbs, L. P.; Weck, M. *Chem.−Eur. J.* **2003**, *9*, 992−999.
(25) Thilbault, R. J.; Hotchkiss, P. J.; Gray, M.; Rotello, V. M. *J. Am. Chem. Soc.* **2003**, *125*, 11249−11252.
(26) Ilhan, F.; Gray, M.; Rotello, V. M. *Macromolecules* **2001**, *34*, 2597−2601.
(27) South, C. R.; Higley, M. N.; Leung, K. C.-F.; Lanari, D.; Nelson, A.; Grubbs, R. H.; Stoddart, J. F.; Weck, M. *Chem.−Eur. J.* **2006**, *12*, 3789−3797.
(28) Albrecht, M.; van Koten, G. *Angew. Chem., Int. Ed.* **2001**, *40*, 3750−3781.
(29) Ashton, P. R.; Campbell, P. J.; Chrystal, E. J. T.; Glink, P. T.; Menzer, S.; Philp, D.; Spencer, N.; Stoddart, J. F.; Tasker, P. A.; Williams, D. J. *Angew. Chem., Int. Ed. Engl.* **1995**, *34*, 1865−1869.
(30) Miecznikowski, J. R.; Gruendemann, S.; Albrecht, M.; Megret, C.; Clot, E.; Faller, J. W.; Eisenstein, O.; Crabtree, R. H. *Dalton Trans.* **2003**, *5*, 831−838.
(31) We assume that the dissociation of the **6-H·BAr$_F$** salt into separated ions would be almost complete in CH_2Cl_2 since the soft BAr_F^- anions are only very weakly associated with the dibenzylammonium cations in **6-H·BAr$_F$** at low dilution. Hence, we report K_a values obtained directly from the ITC experiments on the assumption that ion-pair formation is not prevalent under the reaction conditions. When ion-pairing is significant, it is necessary to invoke a more involved treatment of the ITC data. See: Jones, J. W.; Gibson, H. W. *J. Am. Chem. Soc.* **2003**, *125*, 7001−7004.

MA060314S